Characterization, Signaling, Capacity and Coding Based on Fading Channels: A Review

Zhongli Wang[1], Guo Sheng[2], and Xu Zhang[3]
[1] College of Electrical and Information Engineering, Beihua University, Jilin 132013, China
[2] Department of Communication Engineering, Zhejiang Post and Telecommunication College, Shaoxing 312016, China
[3] Department of Mechanical Engineering and Materials Science, Duke University, Durham, USA
Email: wqwaszx13579@163.com; sg@zptc.cn; xuzhangduke@gmail.com

Abstract —In this paper, the characterization, diversity, signaling, capacity and coding associated with fading channels are reviewed in an intuitive manner. We first introduce the basic concepts of fading and fading hannels with an adequate number of derivations and simulations, by which the effects of fading on wireless communication can be analyzed comprehensively. Then, we also give the performance analysis of signals propagating over flat and slow Rayleigh fading channel as an example. Specifically, the general form of error probability of received signal propagating over such a channel is presented and several special cases are discussed in depth with simulations. After this, we focus on diversity techniques, a powerful tool to overcome deep fading and improve the reliability of wireless communication. In addition, information-theoretic issues, e.g. channel capacity, outage probability and coding based on fading channels are also expatiated. By reading this paper, the readers are expected to have a broad understanding of fading phenomenon, a variety of types of fading channels, effects of fading on wireless communication and the methodologies to overcome the disadvantageous effects. Meanwhile, we also point out the future potential research directions in the relevant fields.

Index Terms—Fading, fading channel, diversity, channel capacity

I. Introduction

Wireless communication has become one of the most vibrant and dynamic research areas in electrical engineering [1]. In recent decades, wireless communication has eased people's life dramatically and a series of novel mobile terminal devices, e.g. smartphone, tablets and laptop, have been ubiquitous [2]. However, until now, fading is still one of the main obstacles preventing the development of communication engineering [3]. The reason is that deep fading degrades the reliability of the communication systems and sometimes even makes the wireless communication impossible [4]. Therefore, the research into fading is of high importance and attracts a large number of researchers' interest in the relevant fields [5]. In addition, fading channel is an important concept different from traditional channel models. Conventionally, to simplify the analysis of communication system and its performance, we simply use a classical Additive White Gaussian Noise (AWGN) channel model with a fixed attenuation factor or a linear filter with a fixed frequency response to model a communication channel [6]. However it is not always the case in practice [7]. In fact, a more complex and general channel model should consider the time-varying property, i.e. the randomness of the channel condition, e.g. path loss and shadowing, as well as the multipath effect [8]. This channel model is called fading multipath channel or simply fading channel. Due to the significance of fading and fading channel, we introduce, review and analyze them and the relevant techniques in depth in this paper. Moreover, we also point out the research directions worth further investigating in the relevant field in this paper.

The rest of this paper is organized as follows. Section II first introduces the fundamentals of fading and fading channels as well as their physical characteristics and mathematical models. Then, a crucial technique, diversity, is explained in Section III. Also, the signaling techniques of fading channel, as the important technique to transmit and receive signals, are analyzed and discussed in Section IV. As for the information theoretic issues, the capacity, outage probability and coding techniques are subsequently detailed in Section V. Finally, we conclude this paper and point out the future research directions in Section VI.

II. Fundamentals of Fading and Fading Channel

A. Basic Concepts and Explanations of Fading and Fadingchannels

The most distinctive characteristics of fading channel is the randomness of channel condition and the multipath effect, which are also known as time-varying property and time spread respectively [9]. The former is used to characterize the randomness of the frequency response of a fading channel [10]. That is, when the same pulse is transmitted for many times, for each time, we measure it and will almost surely receive a different scaled and delayed version of the original transmitted signal. This can be vividly depicted in Fig. 1. The latter is caused by signal reflection, diffraction and scattering [11]. By these propagation mechanisms, not only a single path exists between the transmitter and the receiver, instead, a large number of paths exist. Therefore, when a single pulse is transmitted, a train of pulses will be received over such a fading channel. This can be graphically shown in Fig. 2.

Manuscript received January 11, 2016; revised June 20, 2016.
Corresponding author email: sg@zptc.cn.
doi:10.12720/jcm.11.6.523-538

Therefore, consider both characteristics jointly. The typical form of received random pulse train corresponding to the transmitted signal over the fading channel is shown in Fig. 3.

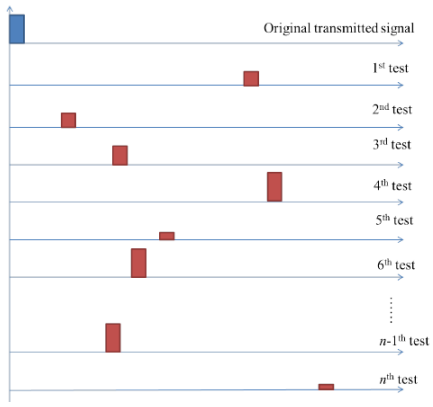

Fig. 1. Time-varying property of a fading channel without considering time spread.

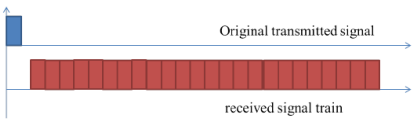

Fig. 2. Time spread of a fading channel without considering time-varying property.

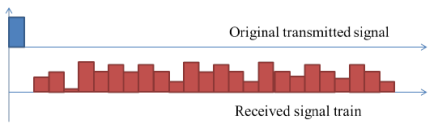

Fig. 3. Typical received pulse train considering time-varying property and time spread of a fading channel.

As can be seen from Fig. 3, the transmitted signal is far harder to recover when propagating over the fading channel than other linear and time-invariant channels [12]. To model these random behaviors, statistical models and tools can be helpful. Consider the general form of modulated signals [13]:

$$s(t) = \mathrm{Re}[s_l(t)e^{j2f_c t}] \tag{1}$$

where $s(t)$ is the equivalent baseband transmitted signal; f_c is the central frequency specified by a certain modulation scheme.

Assume there exist N multiple prorogation paths with random and time-variant channel attenuation factor $\{\alpha_n(t)\}$ and delay $\{\tau_n(t)\}$, where $n \in \{1, 2, \cdots, N\}$. The general form of bandpass received signal without consideration of channel noise can be mathematically expressed as [6]:

$$r(t) = \sum_{n=1}^{N} \alpha_n(t) s[t-\tau_n(t)] \tag{2}$$

Substituting (1) into (2) yields:

$$\begin{aligned} r(t) &= \sum_{n=1}^{N} \alpha_n(t)\,\mathrm{Re}\left\{s_l[t-\tau_n(t)]e^{j2\pi f_c[t-\tau_n(t)]}\right\} \\ &= \mathrm{Re}\left\{\left(\sum_{n=1}^{N} \alpha_n(t)e^{-j2\pi f_c\tau_n(t)} s_l[t-\tau_n(t)]\right)e^{j2\pi f_c t}\right\} \end{aligned} \tag{3}$$

From (3), it is obvious that the equivalent baseband received signal is

$$r_l(t) = \sum_{n=1}^{N} \alpha_n(t)e^{-j2\pi f_c\tau_n(t)} s_l[t-\tau_n(t)] \tag{4}$$

Because $r_l(t) = s_l(t) * c(\tau, t)$, the time-variant impulse response [8] is

$$c(\tau,t) = \sum_{n=1}^{N} \alpha_n(t)e^{-j2\pi f_c\tau_n(t)}\delta[t-\tau_n(t)] \tag{5}$$

Besides, we can also assume $\theta_n(t) = -2\pi f_c \tau_n(t)$ and (6) becomes

$$c(\tau,t) = \sum_{n=1}^{N} \alpha_n(t)e^{j\theta_n(t)}\delta[t-\tau_n(t)] \tag{6}$$

In addition, if the number of paths, i.e. N tends to infinity, we might as well use integral to express (3) and thus obtain [8]:

$$r(t) = \mathrm{Re}\left\{\left[\int_{-\infty}^{\infty} \alpha(\tau,t)e^{-j2\pi f_c\tau} s_l(t-\tau)d\tau\right]e^{j2\pi f_c t}\right\} \tag{7}$$

Therefore, the corresponding time-variant impulse response is

$$c(\tau,t) = \alpha(\tau,t)e^{-j2\pi f_c\tau} \tag{8}$$

where $c(\tau,t)$ is the impulse response of the fading channel at time t to an impulse applied at time $t-\tau$.

Additionally, we can also assume $\theta = -2\pi f_c \tau$ and (8) becomes

$$c(\tau,t) = \alpha(\tau,t)e^{j\theta} \tag{9}$$

Now, let us take a close look at the effects of fading channel on the received signal. Without considering initial value and channel noise, assume an all-one pulse as shown infra is transmitted:

$$s_l(t) = 1, \quad \forall t \in \mathbb{R} \tag{10}$$

Then substituting (10) into (4), for the discrete fading channel mode given in (6), we have the equivalent baseband received signal:

$$\begin{aligned} r_l(t) &= \sum_{n=1}^{N} \alpha_n(t)e^{j\theta_n(t)} \\ &= \sum_{n=1}^{N} \alpha_n(t)\cos\theta_n(t) + j\sum_{n=1}^{N} \alpha_n(t)\sin\theta_n(t) \end{aligned} \tag{11}$$

From (11), it is obvious that the resultant received signal would fluctuate tempestuously due to the alternate constructive and destructive superpositions of received signals from multiple paths with random and time-variant multiplicative factor $\alpha_n(t)e^{j\theta_n(t)}$. This phenomenon is termed signal fading [8]. To sum up, the primary cause of signal fading is due to the time-variant multipath characteristics of the fading channel [9]. Moreover, it can be proved that $\theta_n(t) \sim U(0, 2\pi)$ and the distribution of the angle can be viewed as independent of $\tau_n(t)$ [14]; $\alpha_n(t)$ is distributed as Weibull distribution [15]. Besides, by central limit theorem, it can be further proved that

$$\sum_{n=1}^{N}\alpha_n(t)\cos\theta_n(t) \sim N\left(\mu_n,\sigma_n\right)$$

$$\sum_{n=1}^{N}\alpha_n(t)\sin\theta_n(t) \sim N\left(\mu_n,\sigma_n\right)$$

Therefore, according to the definition of Rayleigh distribution, it is easy to see that r the envelope of the resultant received signal:

$$\left|r_l(t)\right| = \sqrt{\left[\sum_{n=1}^{N}\alpha_n(t)\cos\theta_n(t) \sim N\left(\mu_n,\sigma_n\right)\right]^2 + \left[\sum_{n=1}^{N}\alpha_n(t)\sin\theta_n(t) \sim N\left(\mu_n,\sigma_n\right)\right]^2}$$

is a random Rayleigh distributed variable as long as both Gaussian random components share the same variance. Otherwise, the envelope is Rician distributed. Whether Rayleigh or Rician distribution should be adopted depending on whether there is a Light of Sight (LOS) path between the transmitter and the receiver [16].

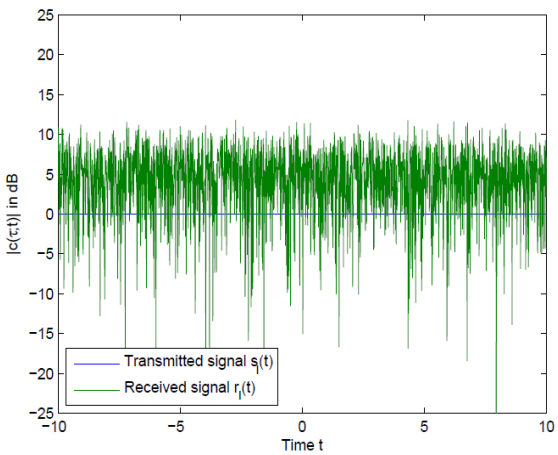

Fig. 4. Amplitude of resultant received signal over Rayleigh fading channel, providing N = 20.

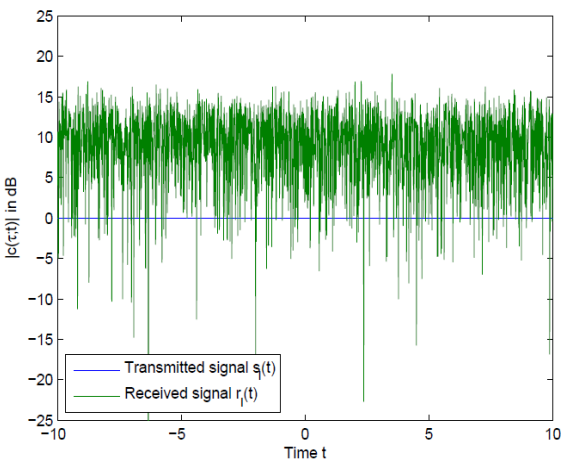

Fig. 5. Amplitude of resultant received signal over Rayleigh fading channel, providing N = 200.

Consider the case of a Rayleigh fading channel, i.e. $\sum_{n=1}^{N}\alpha_n(t)\cos\theta_n(t) \sim N(0,1)$ and $\sum_{n=1}^{N}\alpha_n(t)\sin\theta_n(t) \sim N(0,1)$ with 100 Hz sampling frequency, we can simulate and plot the amplitudes of transmitted signal $s_l(t)$ and the resultant received signal $r_l(t)$ with N = 20, N = 200 and N = 2000 in Fig. 4, Fig. 5 and Fig. 6 respectively. From these three figures, several important features associated with signal fading and multipath fading channel can be found and summarized. First, overall, a multipath fading channel has a positive effect on the signal transmission. Because of the constructive supposition of received signals from multiple paths, in most cases the amplitude of the resultant received signal is larger then the original transmitted signal, which provides a higher Signal-to-Noise Power Ratio (SNR) and thus a better performance than single path channel. Also, with an increasing number of paths, the average amplitude of the resultant received signal has been enlarged and the situation of signal fading has also been improved accordingly. However, the detrimental effect of a multipath fading channel should not be overlooked. As we can see from these figures, the amplitude of the resultant received signal is frequently lower than the amplitude of the transmitted signal, which will result in a degradation of the performance of communication systems. This degradation is termed deep fading and has a significant and negative impact on the system reliability, especially for received signals with memory [8]. To make our summary more reliable, we can also plots the Probability Density Functions (PDF) of these three cases in Fig. 7 and they further validate our analysis.

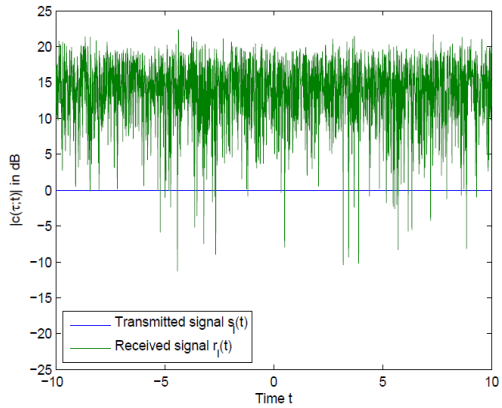

Fig. 6. Amplitude of resultant received signal over Rayleigh fading channel, providing N = 2000.

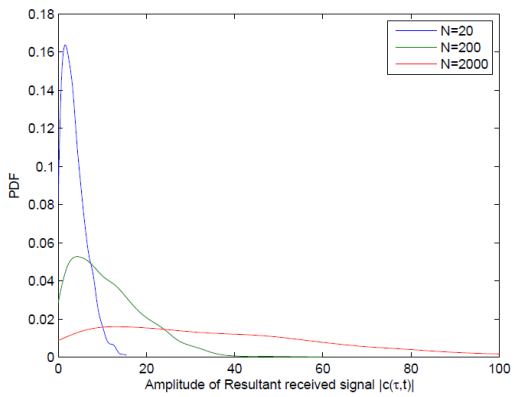

Fig. 7. PDF of amplitude of resultant received signal over Rayleigh fading channel with different number of paths.

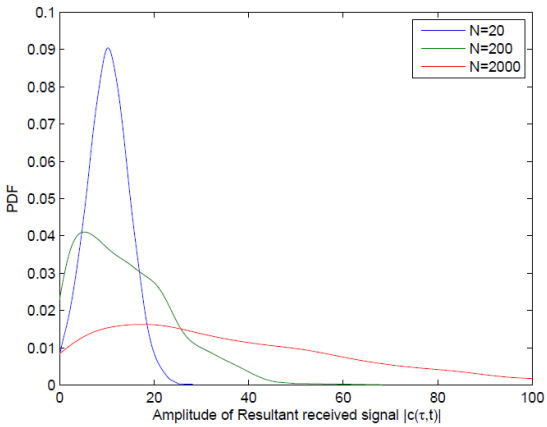

Fig. 8. PDF of amplitude of resultant received signal over Rician fading channel with different number of paths.

Based on this analysis of Rayleigh fading channel, we can easily discuss the scenario when there exists a LOS path. In this case, we should use Rician fading channel model. For the simplification and demonstration purposes, we can simply assume the amplitude of the received signal from LOS path is distributed as $N(10;\ 1)$, whereas the amplitudes of other received signals from N indirect paths are distributed as $N(0;\ 1)$. By this simulation configuration, we can simulate and plot the PDF of the amplitude of resultant received signal over Rician fading channel in Fig. 8. From this figure, it is clear that with a LOS path, the overall performance of the signal transmission can be improved, but with an increasing number of paths, this improvement effect is weakened.

B. *Time Domain and Frequency Domain Properties of Fading Channels*

Based on the assumptions of wide-sense-stationary (WSS) channel and the uncorrelated scattering, i.e. the received signals from different paths with different delays can be regarded as statistically uncorrelated in terms of attenuation and phase shift, we can thus calculate the autocorrelation function of $c(\tau,t)$ by [8]:

$$\begin{aligned} R_c(\tau_2,\tau_1;\Delta t) &= E\left[c^*(\tau_1;t)c(\tau_2;t+\Delta t)\right] \\ &= R_c(\tau_1;\Delta t)\delta(\tau_2-\tau_1) \end{aligned} \tag{12}$$

where τ_1 and τ_2 are the time delays of two received signals transmitted at time $t+\Delta t$ and t, respectively.

If we assume two signals are transmitted at the same time and received with a time difference τ, then the multipath intensity profile or called delay power spectrum of the channel can be defined as [8]:

$$R_c(\tau;0) = R_c(\tau) \tag{13}$$

Also, we can define the multipath spread T_m of a channel as [8]:

$$\exists\,\tau \in (0,T_m)\ \text{ s.t. }\ R_c(\tau) \neq 0 \tag{14}$$

In order words, the variable T_m characterizes the time spread of a channel and once a sharp and narrow pulse is sent, the received signals could spread within (0, T_m) in time domain [17]

Additionally, if we define the channel frequency response as [18]:

$$C(f;t) = \int_{-\infty}^{\infty} c(\tau;t)e^{-j2\pi f\tau}d\tau \tag{15}$$

Based on this definition, analogously, we can define the autocorrelation function of two frequency responses with different carrier frequencies, termed spaced-frequency spaced-time correlation function of a channel [8]:

$$\begin{aligned} R_C(f_2,f_1;\Delta t) &= E\left[C^*(f_1;t)C(f_2;t+\Delta t)\right] \\ &\equiv R_C(\Delta f;\Delta t) \end{aligned} \tag{16}$$

where $\Delta f = f_2 - f_1$.

Similarly, if there is no difference between transmission time instants of two signals, we have

$$R_C(\Delta f,0) \equiv R_C(\Delta f) = \int_{-\infty}^{\infty} R_c(\tau)e^{-j2\pi\Delta f\tau}d\tau \tag{17}$$

We ditto define the coherence bandwidth of a channel as [8]:

$$\exists\, f \in (-\Delta f_c/2, \Delta f_c/2)\ \text{ s.t. }\ R_C(\Delta f) \neq 0 \tag{18}$$

According to (14), (17) and (18), we can approximate the coherence bandwidth of a fading channel [19]:

$$\Delta f_c \approx \frac{1}{T_m} \tag{19}$$

That is, if the carrier frequencies of two transmitted signals are separated larger than Δf_c, they will be affected differently when propagating over the wireless fading channel in terms of attenuation factors and phase shifts and can be viewed as statistically uncorrelated. Assuming W is the bandwidth of the channel, if $\Delta f_c \ll W$, the fading channel is termed frequency-selective fading channel, in which a small variation of carrier frequency of the transmitted signal will result in a significant difference of the amplitude and phase shift of the received signal [20]. Otherwise, the channel is termed frequency-nonselective fading channel or flat fading channel, which indicates all signals with different carrier frequencies are treated without bias [21].

Also, the difference of transmission time between two transmitted signals denoted by Δt, will also matter. To analyze this effect, we should first define the Fourier transform of $R_C(\Delta f;\Delta t)$ with respect to Δt as [8]:

$$S_C(\Delta f;\lambda) = \int_{-\infty}^{\infty} R_C(\Delta f;\Delta t)e^{-j2\pi\lambda\Delta t}d\Delta t \tag{20}$$

Without considering the difference between carrier frequencies, we can define the Doppler power spectrum of a channel as [8]:

$$S_C(0;\lambda) \equiv S_C(\lambda) = \int_{-\infty}^{\infty} R_C(0;\Delta t)e^{-j2\pi\lambda\Delta t}d\Delta t \tag{21}$$

We ditto define the Doppler spread of a channel as [8]:

$$\exists\,\lambda \in (-B_d/2, B_d/2)\ \text{ s.t. }\ S_C(\lambda) \neq 0 \tag{22}$$

From the definition of Doppler spread of a channel B_d, we can define the coherence time of a channel as [19]:

$$\Delta t_c \approx \frac{1}{B_d} \tag{23}$$

This variable Δt_c characterizes the time domain property of the fading channel. That is, if the difference between the transmission time of two signals is greater than Δt_c, they will be treated differently by the channel in terms of attenuation factor and phase shift and can be regarded as statistically uncorrelated [22]. If $\Delta t_c \ll E[\tau]$, the channel is termed fast fading channel; otherwise, it is termed slow fading channel [8].

Overall, we can conclude that if the channel condition $T_m B_d \ll 1$ is satisfied, it is possible to transmit a signal over this channel with flat time and frequency responses [8].

Finally, based on the analysis in this subsection, we can summarize the scattering function of a fading channel with time delay τ and Doppler frequency shift λ by [8]:

$$S_C(\tau;\lambda) = \int_{-\infty}^{\infty}\int_{-\infty}^{\infty} R_C(\Delta f;\Delta t) e^{-j2\pi\lambda\Delta t} e^{j2\pi\tau\Delta f} d\Delta t d\Delta f \tag{24}$$

The variable $S_C(\tau;\lambda)$ can be used to measure the average power output of a fading channel.

C. Statistical Models of Fading Channels

Although the fading channel has been referred many times as $c(\tau;t)$ in the previous sections, we have not constructed the model of its generic form and the selection of parameters systematically. Therefore, in this subsection, we will dig into and construct its mathematical expressions.

The most common case of a fading channel is that there exist a large number of multiple indirect paths between the transmitter and the receiver. In this case, as analyzed before, the envelope of the channel frequency response is Rayleigh distributed and the phase angle is uniformly distributed ranging from 0 to 2π Although Rayleigh distribution is simple and easy to implement, it only contain a single characteristic parameter, which makes it sometimes inaccurate. Because the applicability of Rayleigh distribution for envelop modeling is based on the central limit theorem, if the number of multiple paths reduces, the Rayleigh distribution will become inaccurate and cannot fit the fading channel well [23]. In this case, Nakagami-m distribution, as a two-parameter distribution, would provide a better fit for wireless fading channel modeling [24].

In addition of a relatively infrequent case [25], if there is a LOS path between the transmitter and the receiver, Rician distribution would be proper to use for fading channel modeling, because it takes the unfairness of the received signals from multiple paths into consideration [26].

For a special case in which a LOS path and a small number of indirect paths exist, we can use some simplified and closed forms to model the channel impulse response $c(\tau;t)$. For example, consider the airplane to ground communication as shown in Fig. 9. There are only two multipath components between the transmitter and the receiver, which are LOS path (marked in blue) component and a single multipath component (marked in red) owing to terrian reflections. In this case, the channel impulse response can be expressed as [8]:

$$c(\tau;t) = \alpha\delta(\tau) + \beta(t)\delta\left[\tau - \tau_0(t)\right] \tag{25}$$

where α is a constant attenuation factor of the LOS path; $\beta(t)$ is the time-variant attenuation factor of the single indirect path; $\tau_0(t)$ is the time-variant path delay of the single indirect path. According to (15) and (25), we have:

$$C(f;t) = \alpha + \beta(t) e^{-j2\pi f \tau_0(t)} \tag{26}$$

Based on (26), a more sophisticated and specific model used for microwave LOS radio channel of long-distance signal transmission can be constructed as below [27]:

$$C(f) = \alpha\left[1 - \beta e^{-j2\pi(f-f_0)\tau_0}\right] \tag{27}$$

where α is a overall attenuation parameter; β is the shape parameter caused by multipath components; f_0 is the frequency of the fade minimum; τ_0 is the relative time delay between the LOS path and the indirect path.

In this model, we assume that the difference of time delays among different indirect paths is rather small in comparison with the time delay between the LOS path and any indirect path. Also, it is clear that this model is an approximation of time-invariant channel model and can ease the analysis for this special case.

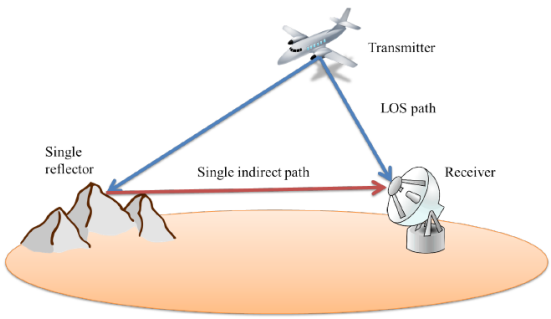

Fig. 9. Airplane to ground communication model.

D. Performance Analysis of Signals Propagating over Flat and Slow Fading Channel

As long as $T_m B_d \ll 1$, it could be proved that signals transmitted over a flat and slow fading channel will experience a multiplicative distortion with random but time-invariant attenuation factor and phase shift within one or multiple signaling intervals [8]. Therefore, consider the equivalent baseband signal model given above. Within a signaling interval [0, T], we have

$$r_l(t) = \alpha e^{j\phi} s_l(t) + z(t) \tag{28}$$

where α is the constant attenuation factor; ϕ is the phase shift; $z(t)$ is the complex-valued AWGN term.

Because the signals are transmitted over flat and slow fading channel, the channel frequency response, i.e. $\alpha e^{j\phi}$ can be estimated easily by pilot signals or training

sequences [28], [29]. Hence, we can use matched filter and coherent detection techniques to determine the received signal $r_l(t)$ [30]. Obviously, the error probability of coherent detection only depends on the randomness of the attenuation factor. Assuming for a fixed attenuation factor, the error probability is denoted as $P_b(\alpha)$. Then, if the attenuation factor is random and distributed by a PDF $p_\alpha(\alpha)$ average error probability can be expressed by [31]:

$$\begin{aligned} P_b &= E\left[P_b(\alpha)\right] = \int_\alpha P_b(\alpha) p_\alpha(\alpha) d\alpha \\ &= \int_0^\infty P_b(\alpha) p_\alpha(\alpha) d\alpha \end{aligned} \tag{29}$$

Meanwhile, by fundamentals of signal processing [18], we can also use SNR per bit to express the relations given above:

$$\gamma_b = \frac{\alpha^2 \varepsilon_b}{N_0} \tag{30}$$

where ε_b is the energy in each information bit; N_0 is the power spectral of complex-valued AWGN.

Therefore, based on the relation given in (30), (29) can be rewritten as:

$$\begin{aligned} P_b &= E\left[P_b(\gamma_b)\right] = \int_{\gamma_b} P_b(\gamma_b) p_{\gamma_b}(\gamma_b) d\gamma_b \\ &= \int_0^\infty P_b(\gamma_b) p_{\gamma_b}(\gamma_b) d\gamma_b \end{aligned} \tag{31}$$

For BPSK signal, the fixed attenuation error probability is [32]:

$$P_{b-BPSK}(\gamma_b) = Q\left(\sqrt{2\gamma_b}\right) \tag{32}$$

where $Q(\cdot)$ is the tail probability of the standard normal distribution.

Further assume that the transmitted signal propagates over a flat and slow Rayleigh fading channel. We can determine the PDF of α [33]:

$$p_\alpha(\alpha) = \begin{cases} \dfrac{\alpha}{\sigma^2} e^{-\frac{\alpha^2}{2\sigma^2}}, & \alpha > 0 \\ 0, & \text{otherwise} \end{cases} \tag{33}$$

where σ equals to 1 for standard Gaussian random process [33].

Due to (30) and (33), we have:

$$p(\gamma_b) = \frac{1}{\bar{\gamma}_b} e^{-\gamma_b/\bar{\gamma}_b}, \quad \gamma_b \geq 0 \tag{34}$$

where $\bar{\gamma}_b = \varepsilon_b E(\alpha^2)/N_0$.

Also, for a standard Gaussian random process, we can determine $E(\alpha^2)$ by [8]:

$$\begin{aligned} E(\alpha^2) &= \mathrm{var}(\alpha) + \left[E(\alpha)\right]^2 \\ &= \left(2 - \frac{\pi}{2}\right)\sigma^2 + \left(\sigma\sqrt{\frac{\pi}{2}}\right)^2 = 2 \end{aligned} \tag{35}$$

According to (29), (32) and (34), we can obtain the average error probability for BPSK [8]:

$$P_{b-BPSK} = \frac{1}{2}\left(1 - \sqrt{\frac{\bar{\gamma}_b}{1+\bar{\gamma}_b}}\right) \tag{36}$$

Following a similar derivation procedure of the BPSK case, for BFSK with coherent detection, BFSK with noncoherent detection and DPSK, we have [8]:

$$P_{b-BFSK(C)} = \frac{1}{2}\left(1 - \sqrt{\frac{\bar{\gamma}_b}{2+\bar{\gamma}_b}}\right) \tag{37}$$

$$P_{b-BFSK(NC)} = \frac{1}{2+\bar{\gamma}_b} \tag{38}$$

$$P_{b-DPSK} = \frac{1}{2(1+\bar{\gamma}_b)} \tag{39}$$

Based on these relations derived above, we can simulate and plot the results in Fig. 10. From this figure, it is clear that BPSK outperforms other three signaling schemes due to its constant envelope property, i.e. $|s_{l1}(t)| = |s_{l2}(t)|$. It can also be observed that the performances of BFSK with coherent detection and DPSK are similar, especially when SNR is relatively high. However, because the channel state is not estimated by noncoherent detection, the BFSK with noncoherent detection has the worst performance in comparison with other three signaling schemes [8].

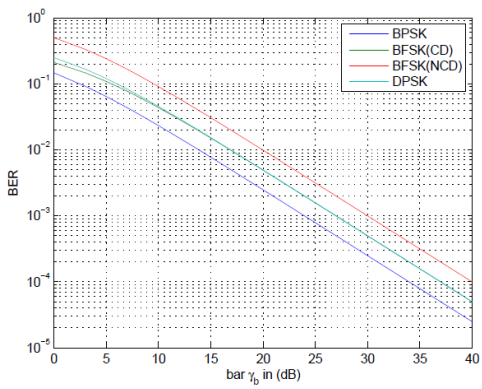

Fig. 10. Relations between $\bar{\gamma}$ and P_b for BPSK, BFSK with coherent detection, BFSK with noncoherent detection and DPSK.

III. Diversity and Receiving Techniques for Signals Transmitted Over Fading Channels

A. Concept and Classification of Diversity

As the transmission and signaling techniques have been analyzed in the previous section, we focus on diversity and receiving techniques of signals transmitted over fading channels in this section.

Diversity technique is based on the viewpoint that if a large number of replicas of the same signal are transmitted, even though several replicas experience deep fading and are severely distorted when received, the transmitted signal is still recoverable from the combination of all replicas [34]. This idea is feasible,

because fading channels of different signal replicas are statistically independent, simultaneous deep fading for all signal replicas is almost surely impossible as long as the number of signal replicas is sufficiently large. Theoretically, the performance and reliability of the communication system can be improved by this way. By fundamental statistics [33], assuming p_f is the probability of the occurrence of deep fading of a transmitted signal replica and the number of replicas is L, we can determine the probability of the event that all signal replicas are deep faded over statistically independent fading channels is

$$p_{fL} = \prod_{l=1}^{L} p_f = p_f^L \tag{40}$$

As the merit of diversity has been analyzed, it is the time to move forward to the implementation of diversity techniques. There are a number of approaches to provide diversity for the receiver, e.g. frequency diversity, time diversity and space diversity. For frequency diversity, we can employ a set of L carriers with frequency separation greater than Δf_c and thus they are statistically uncorrelated when received [35]. Alternatively, time diversity can also be utilized. To achieve time diversity, we can also transmit signal replicas by L time slots with a time separation greater than Δt_c [36]. As for space diversity, it is also known as antenna diversity and utilizes multiple antennas to transmit and receive signal replicas [37]. To guarantee the feasibility of space diversity, we should ensure different antenna pairs are placed with a sufficiently large distance so that the channels among them can be viewed as statistically independent [8]. More complicated, we can transmit a wideband signal with bandwidth $W \gg \Delta f_c$. Therefore, in different correlated frequency intervals, the frequency components of the entire wideband signal will be treated differently and form a large number of statistically independent signal segments with different central frequencies at the receiver [8]. Owing to this statistical independence, they can provide frequency diversity as well. Accordingly, a RAKE correlator or called RAKE matched filter can be applied to receive and detect these signal segments [38].

B. Communication System and Channel with Diversity

Following the assumption of flat and slow Rayleigh fading channel stated in the last section, with such L i.i.d. diversity channels, we can express the equivalent baseband received signal of a M-ary modulation scheme by [39]:

$$r_{lk}(t) = \alpha_k e^{j\phi_k} s_{km}(t) + z_k(t) \tag{41}$$

where $k \in \{1,2,\cdots,L\}$; $m \in \{1,2,\cdots,M\}$; $\{s_{km}(t)\}$ represents the equivalent baseband m-th transmitted signal over the k-th channel; $\alpha_k e^{j\phi_k}$ represents the attenuation factor and phase shift of k-th channel; $z_k(t)$ is the AWGN term of the k-th channel.

Because $\{s_{km}(t)\}$ is manipulated by a certain modulation scheme, it is also known to the receiver. Hence, the receiver can utilize M matched filters with impulse responses infra to detect the received signals [40]:

$$b_{km}(t) = s_{km}^*(T-t) \tag{42}$$

Once the channel can be perfectly estimated, i.e. $\{\alpha_k\}$ and $\{\phi_k\}$ are known to the receiver, the index of transmitted signal m_t can be optimally determined by the algorithm of maximal ratio combination (MRC) as illustrated in (43) [41]:

$$m_t = \arg\max_{m\in\{1,2,\cdots,M\}} \left\{ \sum_{k=1}^{L} \alpha_k e^{-j\phi_k} \int_0^T \left[\alpha_k e^{j\phi_k} s_{m_t}(t) + z_k(t) \right] s_m^* \right\} \tag{43}$$

The multiplicative term $\{\alpha_k e^{-j\phi_k}\}$ shown in this equation is used to compensate the effect of phase shift and ease the elimination of deep faded received signals [8]. Finally, such a detection procedure involving MRC and diversity channels can be summarized in Fig. 11.

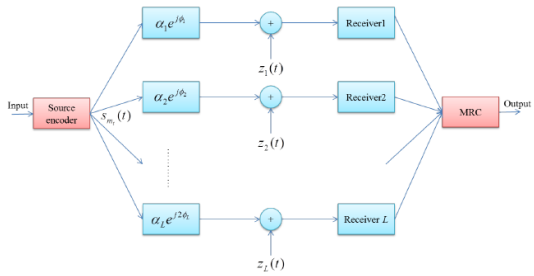

Fig. 11. Detection of received signals propagating over diversity fading channels by MRC [8].

Without loss of generality, we can take BPSK as a specific example to illustrate this procedure in details. Following (31), (32) and (43), we can obtain the average error probability in this case [8]:

$$P_{b-BFSK-L} = \left[\frac{1}{2}\left(1 - \sqrt{\frac{\bar{\gamma}_c}{1+\bar{\gamma}_c}}\right)\right]^L \times \sum_{k=0}^{L-1} \binom{L-1+k}{k} \left[\frac{1}{2}\left(1 + \sqrt{\frac{\bar{\gamma}_c}{1+\bar{\gamma}_c}}\right)\right]^k \tag{44}$$

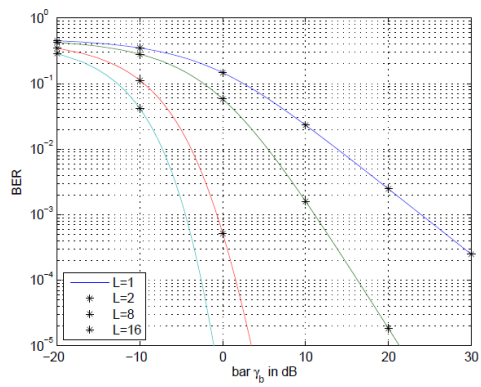

Fig. 12. Error probability of BPSK with different diversity.

In comparison with (36), we can simulate and illustrate the results in Fig. 12. From this figure, some key points can be summarized. First, diversity is a very powerful tool to combat deep fading and improve the reliability of wireless communication systems. However, its feasibility is based on the large SNR. Otherwise, when $\bar{\gamma}_b \ll 1$, the effect of diversity becomes inconspicuous.

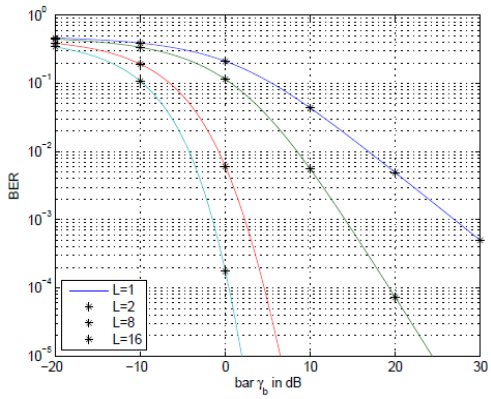

Fig. 13. Error probability of BFSK by coherent detection with different diversity.

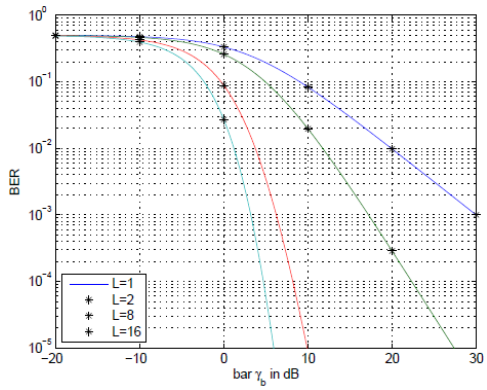

Fig. 14. Error probability of BFSK by noncoherent detection with different diversity.

Similarly, for BFSK with coherent detection, following the derivation procedure of BPSK, we have [8]:

$$P_{b-BFSK(CD)-L} = \left[\frac{1}{2}\left(1-\sqrt{\frac{\bar{\gamma}_c}{2+\bar{\gamma}_c}}\right)\right]^L \times \sum_{k=0}^{L-1}\binom{L-1+k}{k}\left[\frac{1}{2}\left(1+\sqrt{\frac{\bar{\gamma}_c}{2+\bar{\gamma}_c}}\right)\right]^k \tag{45}$$

Simulation of (45) using MATLAB yields the results shown in Fig. 13.

Likewise, for BFSK with noncoherent detection, following the derivation procedure of BPSK, we have [8]:

$$P_{b-BFSK(NCD)-L} = \left[\frac{1}{2}\left(1-\frac{\bar{\gamma}_c}{2+\bar{\gamma}_c}\right)\right]^L \times \sum_{k=0}^{L-1}\binom{L-1+k}{k}\left[\frac{1}{2}\left(1+\frac{\bar{\gamma}_c}{2+\bar{\gamma}_c}\right)\right]^k \tag{46}$$

Simulation of (46) using MATLAB yields the results shown in Fig. 14.

Analogously, for DPSK, following the deviation procedure of BPSK, we have [8]:

$$P_{b-QPSK-L} = \frac{1}{2^{2L-1}(L-1)!(1+\bar{\gamma}_b)^L} \times \sum_{k=0}^{L-1}\frac{1}{k!}\left[\sum_{n=0}^{L-1-k}\binom{2L-1}{n}\right](L-1+k)!\left(\frac{\bar{\gamma}_c}{1+\bar{\gamma}_c}\right)^k \tag{47}$$

Simulation of (47) using MATLAB yields the results shown in Fig. 15.

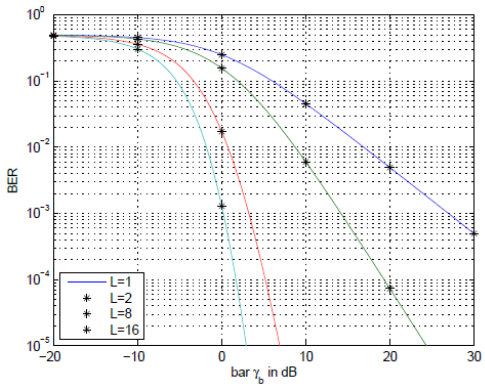

Fig. 15. Error probability of DPSK by noncoherent detection with different diversity.

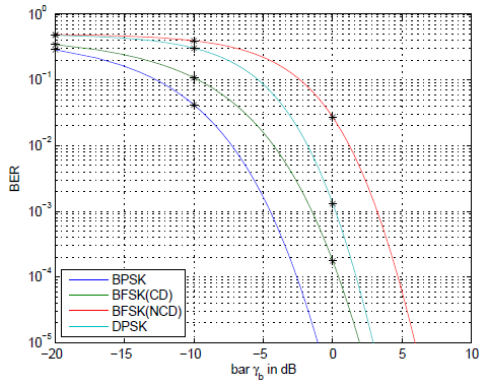

Fig. 16. Comparison among BPSK, BFSK(CD), BFSK(NCD) and DPSK with L=16 diversity channels.

It is not surprising that all modulation schemes presented above follow the same trend when diversity technique is employed. This consistency validates the practicability and universality of diversity as well as its advantageous effects. That is, whichever modulation scheme is used, diversity will always improve the reliability of the communication system and with different SNR, the improvement effect could be obvious or trivial. Now let us move our attention to the comparison among different modulation schemes with the same number of diversity channels, say L=16. The comparison results are illustrated in Fig. 16. From this figure and Fig. 10, we can find that although the advantageous effects of diversity are suited for all of these four modulation schemes, BFSK with coherent detection obtains a more obvious improvement when

diversity technique is performed and the improvement of BPSK with noncoherent detection is relatively small.

IV. Signaling Techniques of Frequency-Selectiive Fading Channels

A. Wideband Signal and Tapped Delay Line Channel Model

In order to obtain diversity and overcome deep fading, the basic signaling philosophy of transmitted signal over fading channels can be described as follows. Either modulating a signal so that it has a bandwidth $W \ll \Delta f_c$ or subdividing its entire bandwidth W so that each subdivision has a bandwidth $W_s \ll f_c$. Alternatively, a more intuitive and convenient way to achieve this goal is to employ a wideband signal with bandwidth $W \gg \Delta f_c$ and transmission pulse interval $T \ll t_c$ [8]. In this case, the fading channel can be viewed as a frequency-selective and slow fading channel. The frequency components of the transmitted signal over this channel are treated differently but the channel frequency response is WSS. By sampling theory, such a wideband signal has a equivalent baseband signal as expressed below:

$$s_l(t) = \sum_{n=-\infty}^{\infty} s_l\left(\frac{n}{W}\right)\frac{\sin\left[\pi W(t-n/W)\right]}{\pi W(t-n/W} \tag{48}$$

For such a transmitted signal, according to (3) and (48), the noiseless equivalent baseband received signal over a frequency-selective facing channel can be expressed as:

$$r_l(t) = \frac{1}{W}\sum_{n=-\infty}^{\infty} s_l\left(t-\frac{n}{W}\right)c\left(\frac{n}{W},t\right) \tag{49}$$

As long as the number of subchannels is large enough, for each frequency interval 1=W, the channel frequency response can be regarded as flat and the channel impulse response can be viewed as only depending on time t and thus we have the expression given infra [8]:

$$c_n(t) = \frac{1}{W}c\left(\frac{n}{W},t\right) \tag{50}$$

This provides a foundation for us to model the fading channel as a filter with a number of taps. In practice, the number of filter taps is a finite value and thus a filter system with infinite taps should be truncated for implementation purpose. Let $L = \lfloor T_m W \rfloor + 1$ and the truncated tapped delay line channel model can be expressed by [18]:

$$r_l(t) = \sum_{n=1}^{L} c_n(t) s_l\left(t-\frac{n}{W}\right) \tag{51}$$

In accordance with the aforementioned assumptions of uncorrelated scattering and the specification of wideband signal, the tap coefficients $c_n(t)$ is statistically independent and time-variant. Therefore, L signal replicas are provided and form a diversity for the receiver. This truncated tapped delay line channel model can also be graphically depicted in Fig. 17. By this way, the reliability of the communication system can be improved by employing wideband signals.

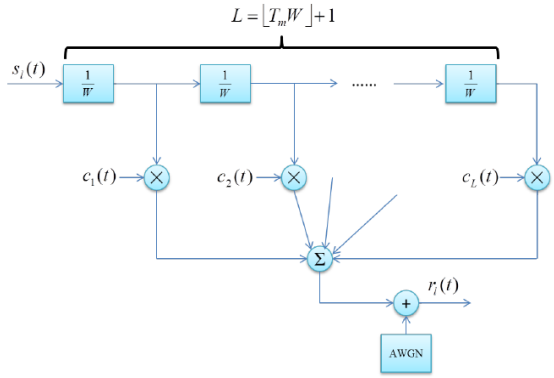

Fig. 17. Tapped delay line model of frequency-selective fading channels [8].

B. RAKE Demodulator

As we mentioned in Section III, RAKE demodulator is a powerful tool to process multiple signal replicas and detect the wideband signal. In this subsection, it will be analyzed in details.

For the simplification and demonstration purposes, we might first consider M-ary signaling scheme consisting of M homenergic signal waveforms $\{s_{lm}(t)\}$ over the frequency selective fading channel, where $m \in \{1,2,\cdots,M\}$. As the specification of wideband signals, the intersymbol interference (ISI) caused by multipath effect can be ignored, since the transmission pulse interval T of a wideband signal is far greater then the time spread T_m. Because we also assume $T \ll \Delta t_c$, the fading channel varies slowly compared to the transmitted signal. As a consequence, it is reasonable to assume the fading channel can be estimated perfectly and thus $\{c_n(t)\}$ is know to the receiver. According to (43) and assuming the index of transmitted signal is m_t, the detection procedure of RAKE demodulator can be expressed in (52). This detection procedure involving RAKE demodulator can also be graphically depicted in Fig. 18. On the other hand, if ISI is not negligible, a channel equalizer could be inserted between the sampler and the integrator to compensate the nonlinear effect caused by ISI [8].

$$\begin{aligned} m_t &= \arg\max_{m\in\{1,2,\cdots,M\}}\left\{\int_0^T r_l(t)\left[\sum_{k=1}^{L} c_k^*\left[T-(\tau-t)\right]s_{lm}^*\left[T-\left(\tau-t+\frac{k}{W}\right)\right]\right]dt\right\}_{\tau=T} \\ &= \arg\max_{m\in\{1,2,\cdots,M\}}\left\{\int_0^T\left[\sum_{k=1}^{L} c_k(t)s_{lm_t}\left(t-\frac{k}{W}\right)+z(t)\right]\left[\sum_{k=1}^{L} c_k^*\left[T-(\tau-t)\right]s_{lm}^*\left[T-\left(\tau-t+\frac{k}{W}\right)\right]\right]dt\right\} \end{aligned} \tag{52}$$

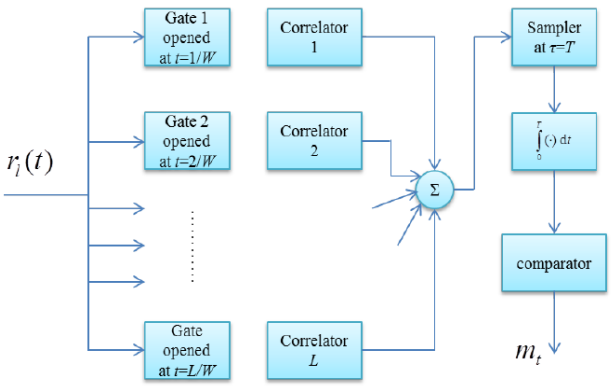

Fig. 18. RAKE demodulator model [19].

C. Orthogonal Frequency Division Multiplexing (OFDM) Over Fading Channels

For the time being, due to the excellent immunity against ISI and the high bandwidth efficiency, Orthogonal Frequency Division Multiplexing (OFDM) is the core of 4G mobile communication network and the most promising technique in communication engineering [42]–[44]. However, the time varying property of fading channel would bring a severe damage for the carrier orthogonality and thereby degrade the performance of OFDM by interchannel interference (ICI) [8]. In order to implement OFDM over fading channels, it is necessary to analyze its performance systematically and figure out the influencing mechanism of ICI. To do so, we should first construct the fundamental model of an OFDM system.

In general, N subcarriers $\{e^{j2\pi f_k t}\}$ are employed to construct an OFDM multicarrier system, where $k \in \{1,2,\cdots,N\}$ and $\Delta f = f_{k+1} - f_k = 1/T$ T is the symbol duration. The carrier orthogonality can be expressed as:

$$\forall \ i \in \{1,2,\cdots N\} \bigcap \{i \neq k\}$$
$$\exists \ \frac{1}{T}\int_0^T e^{j2\pi f_i t} e^{j2\pi f_k t} dt = \begin{cases} 1, \ i = k \\ 0, \ i \neq k \end{cases} \tag{53}$$

Generally, the number of subcarriers employed in OFDM is sufficiently large so that all of the subchannels can be regarded as flat fading channels. Then, according to (5), we have the general form of the channel impulse response of k-th subchannel [8]:

$$c_k(\tau;\ t) = \alpha_k(t)\delta(\tau) \tag{54}$$

Then, by a series of derivations similar to the derivations presented in Section II, we can obtain the multipath power intensity profile in this case [8]:

$$R_c(\tau) = \beta e^{-\beta\tau} \tag{55}$$

where β is a positive parameter controlling the coherence bandwidth of the subchannel.

By Fourier transform, we can further analyze the correlation of the fading across the subcarriers by:

$$R_C(f) = \mathcal{F}[R_c(\tau)] = \frac{\beta}{\beta + j2\pi f} \tag{56}$$

Having introduced the frequency domain property of OFDM over fading channel, it is the time to move towards time domain property. In general for practical communication systems and channels, we have $T \ll \Delta T_c$ [1]. Therefore, the fading channel can be regarded as slow and WSS during the transmission interval of each OFDM symbol. To model such a slow fading channel, we might use the two-term Taylor series expansion to approximate the channel attenuation factor $a_k(t)$ during each symbol interval $t \in [0,T]$ [45].

$$a_k(t) = a_k\left(\frac{T}{2}\right) + \left(t - \frac{T}{2}\right)a_k'\left(\frac{T}{2}\right) \tag{57}$$

Substituting (57) into (54) yields the general form of channel impulse response of k-th OFDM subchannel within a symbol interval:

$$c_k(\tau;t) = a_k\left(\frac{T}{2}\right)\delta(\tau) + \left(t - \frac{T}{2}\right)a_k'\left(\frac{T}{2}\right)\delta(\tau) \tag{58}$$

Based on (4) and (58), the equivalent baseband received signal can be determined by [8]:

$$\begin{aligned} r_l(t) = &\frac{1}{\sqrt{T}}\sum_{k=1}^{N} a_k\left(\frac{T}{2}\right)s_k e^{j2\pi f_k t} + \\ &\frac{1}{\sqrt{T}}\sum_{k=1}^{N}\left(t - \frac{T}{2}\right)a_k'\left(\frac{T}{2}\right)s_k e^{j2\pi f_k t} + n(t) \end{aligned} \tag{59}$$

where $\{s_k\}$ represents the complex valued signal constellation points stipulated by a certain modulation scheme; $n(t)$ is the AWGN term.

To demodulate these N constellation points contained in the received signal $r_l(t)$, we can simply use N parallel correlators with the correlation frequencies corresponding to the OFDM subcarriers' frequencies [46]. Then the output of i-th correlator can be determined by [8]:

$$\begin{aligned} \hat{s}_i &= \frac{1}{\sqrt{T}}\int_0^T r(t)e^{-j2\pi f_i t} \\ &= \underbrace{a_i\left(\frac{T}{2}\right)s_i}_{\text{Desired signal}} + \underbrace{\frac{T}{2\pi j}\sum_{k=1,k\neq i}^{N}\frac{a_k'(T/2)s_k}{k-i}}_{\text{ICI}} + \underset{\text{Noise term}}{n_i} \end{aligned} \tag{60}$$

In (60), we have separated the effects of the transmitted signal, ICI and noise. Because for slow fading channel, $a_i(t)$ is estimable, we can simply send a scaled version of $\hat{s}_i$ to detector to evaluate the transmitted constellation point of this subcarrier. Involving mean-square values, we can calculate the energy of desired signal and ICI respectively by [47]:

$$S = E\left[\left|a_i(T/2)s_i\right|^2\right] \tag{61}$$

and

$$\begin{aligned} I &= E\left[\left|\frac{T}{2\pi j}\sum_{k=1,k\neq i}^{N}\frac{a_k'(T/2)s_k}{k-i}\right|^2\right] \\ &= \frac{(Tf_m)^2}{2}\sum_{k=1,k\neq i}^{N}\frac{2E\left[\left|a_i(T/2)s_k\right|^2\right]}{(k-i)^2} \end{aligned} \tag{62}$$

where f_m is the maximum Doppler frequency.

Therefore, we can determine the signal-to-interference ratio (SNIR) by:

$$SNIR = \frac{S}{I} = \frac{1}{\frac{(Tf_m)^2}{2}\sum_{k=1,k\neq i}^{N}\frac{1}{(k-i)^2}} \tag{63}$$

Finally, we are able to use (63) as a benchmark to evaluate the performance of an OFDM system in fading channel and quantify the effect of ICI caused by Doppler shift.

V. Capacity and Coding Techniques of Fading Channels

A. Fundamentals of Channel Capacity

In this section, the information-theoretic issues related to fading channels will be discussed. Several important concepts, e.g. ergodic capacity, outage capacity and outage probability, will also be addressed. Considering the properties of fading phenomenon and the time domain properties of different types of fading channels, the calculation of channel capacity should be classified into two different cases. One is the fast fading channel and another is the slow fading channel. For the former case, the channel state varies sharply and vehemently during a single transmission interval of a information block. As a result, during a transmission interval of a single block, all possible channel states will be experienced by the waveforms in the block. Hence, the ergodic channel model and ergodic capacity would be more appropriate to use in this case [46], [48], [49].

For the latter case, the channel state is quasi-static during a transmission interval of a block. Therefore, for different blocks, different channel states will be experienced but within a block, all signal waveforms will be assumed to experience the same channel state. Therefore, capacity in different block transmission interval is different and random. As a consequence, outage capacity should be used to characterize the channel [50]–[52]. More specifically, from information theory, we might know that the channel capacity characterizes the randomness and uncertainty of a channel [53]. Therefore, whether the channel state information (CSI) can be estimated will affect the channel capacity [54]–[56]. As we can see from Fig. 16 of BFSK signals with coherent detection and noncoherent detection, if CSI is unobtainable, the performance for the communication system will be degraded even the same modulation scheme is employed. In general, CSI can be known to the transmitter or the receiver or both [57]. In terms of the transmitting end, CSI can be utilized to dynamically adjust the transmission strategy and thus obtain a better performance and reliability [58]. For example, if the channel is in deep fade or with strong interference, the transmitter might choose to increase the transmitter power or suppress transmission until the channel condition becomes better [59]. In terms of the receiving end, the receiver can use CSI to extract the channel attenuation factor and phase shift so that correlators can be employed to effectively demodulate the received signals [60].

According to information theory founded by Shannon, the concept of channel capacity is defined as the supremum of the transmission rate at which reliable communication over the channel is possible [61]. Otherwise, whatever we design the transmission and detection techniques, we would not be able to obtain reliable communication [8]. That is, as long as the transmission rate is less than channel capacity, we can always find out a coding scheme to achieve an infinitesimal error probability. As definition, the general form of the capacity of a discrete memoryless channel is:

$$C = \max_{p(x)} I(X;Y) \tag{64}$$

where $p(x)$ is the probability of the occurrence of event x, i.e. the information symbol x is transmitted; $I(X; Y)$ is the mutual information between events sets $\mathcal{X}$, i.e. the possible transmitted symbols and $\mathcal{Y}$, i.e. the possible received symbols.

From a practical point of view, for a band-limited power-constrained discrete-time AWGN channel, we might use a reduced version of (64) to determine the channel capacity [8]:

$$C = W\log\left(1-\frac{P_t}{N_0 W}\right) \tag{65}$$

where W is the channel bandwidth; P_t is the transmitter power; N_0 is the power spectral density of complex-valued AWGN.

However, we should also note that the capacity models constructed above are based on the assumption that the number of channel states is infinite. In practice, it is not the case, instead, the channel state is randomly and independently determined from a set of finite possible states. This model is termed finite-state channel model [62]. Such a finite-state channel model with N states can be depicted in Fig. 19. We mainly consider this channel model in the following subsections.

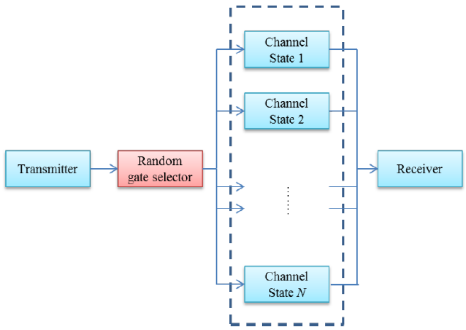

Fig. 19. Finite-state channel model with N states.

B. Ergodic Capacity

From Fig. 19, we can make the concepts of ergodic capacity more explicit. The ergodic capacity $\bar{C}$ should be

used if the random gate selector varies its output selecting index and thereby changes the channel states within one transmission interval of a single block. Also, since this variation is far faster than the transmission interval of a single block, almost all channel states can be experienced for the block, whereas, the outage probability C_ε should be used if the random gate selector maintains its output selecting index during the entire transmission interval. Therefore, only a random channel state will be selected and experienced by the entire block.

Now let us analyze both in details. First, for ergodic capacity, we can assume that the random gate selector outputs selecting index according to a fixed probability density function and the probability of choosing *i*-th channel state with channel capacity $\{C_i\}$ is a fixed value and denoted by $\{\delta_i\}$. Obviously, the relation among all $\{\delta_i\}$, given $i \in \{1, 2, \cdots, N\}$, exists:

$$\sum_{i=1}^{N} \delta_i = 1 \tag{66}$$

Therefore, without CSI, the ergodic capacity of such a channel can be determined by the average of the channel capacities corresponding to all channel states:

$$\bar{C} = \sum_{i=1}^{N} \delta_i C_i = \sum_{i=1}^{N} \delta_i \max_{p(x_i)} I(X_i; Y_i) \tag{67}$$

On the other hand, if CSI is only obtainable at the receiver, then we can determine the ergodic capacity by [8]:

$$\bar{C}_S = \sum_{i=1}^{N} \delta_i \max_{p(x_i)} I(X_i; Y_i \mid S_i) \tag{68}$$

where $\{S_i\}$ represents the known channel state.

In addition, if CSI is obtainable at both transmitter and receiver, we have [63]:

$$\bar{C}_S = \sum_{i=1}^{N} \delta_i \max_{p(x_i|S)} I(X_i; Y_i \mid S_i) \tag{69}$$

Taking the Rayleigh fading channel as an example, for *i*-th state, we can employ the baseband discrete-time equivalent channel model to ease our analysis:

$$y_i = r_i x_i + n_i \tag{70}$$

where $\{x_i\}$ and $\{y_i\}$ represent the complex input and output when the *i*-th channel state has been selected; $\{r_i\} = \{|r_i| e^{j\phi_i}\}$ characterizes CSI of the i-th channel state and can be simply regarded as a complex i.i.d. random variable with Rayleigh distributed magnitude and uniformly distributed phase; $\{n_i\}$ is the i.i.d. complex AWGN term of i-th channel state.

Assuming the transmitted power and received power conserve and equal to P_{tr}, then a parametric expression can be utilized to calculate the ergodic capacity [64]:

$$\begin{aligned} P_{tr} &= \mu e^{-\gamma - \psi(\mu) - 1} \\ \bar{C} &= \frac{\mu - \gamma - \mu\psi(\mu) - 1}{\ln 2} + \log_2 \Gamma(\mu) \end{aligned} \tag{71}$$

where μ is a parameter connecting P and $\bar{C}$ without physical meaning; γ is the Euler's constant; $\Gamma(\cdot)$ is the Gamma function, $\psi(\cdot) = \Gamma'(\cdot)/\Gamma(\cdot)$.

On the other hand, once CSI is detectable at the receiving end, according to (68), the ergodic capacity has a closed form and can be expressed as [8]:

$$\begin{aligned} \bar{C}_S &= \frac{1}{\ln 2} e^{\frac{N_0}{P_{tr}}} \int_{\frac{N_0}{P_{tr}}}^{\infty} t^{-1} e^{-t} dt \\ &\approx \begin{cases} \dfrac{1.44 P_{tr}}{N_0}, & \dfrac{P_{tr}}{N_0} \gg 1 \\ \log\left(\dfrac{P_{tr}}{N_0}\right) - 0.8327, & \dfrac{P_{tr}}{N_0} \ll 1 \end{cases} \end{aligned} \tag{72}$$

Moreover, once CSI is detectable at both transmitting and receiving ends, according to (69), the ergodic capacity has a closed form and can be expressed as [8]:

$$\bar{C}_S = \frac{1}{\ln 2} \int_{\rho_0}^{\infty} t^{-1} e^{-t} dt \tag{73}$$

where ρ_0 is a parameter which satisfies:

$$\int_0^{\infty} \max\left(0, \frac{1}{\rho_0} - \frac{1}{\rho}\right) e^{-\rho} d\rho = \frac{P_{tr}}{N_0} \tag{74}$$

C. Outage Capacity

As the definition of outage channel model, once a channel state is selected, it is assumed to be quasi-static during the entire transmission interval of a block. Therefore, due to the randomness of the gate selector, the channel capacity becomes random before the transmission of a block. However, the transmission rate R is normally constant regardless of the random channel capacity [65]. Therefore, there is a probability that R would exceed the capacity, in which case a outage of the channel will occur. This probability is termed outage probability and can be mathematically expressed by [8]:

$$P_{out}(R) = \Pr[C < R] = \int_{-\infty}^{R} p_C(C) dC \tag{75}$$

where $p_C(C)$ is the PDF of random capacity C.

Theoretically, it is impossible to completely avoid outage as long as a positive transmission rate R is employed. Therefore, it would be wise to set a tolerable threshold of outage probability $\varepsilon \in (0,1)$ and accordingly adjust R to ensure $P_{out}(R) \le \varepsilon$. In this case, the ε-outage capacity can be mathematically defined as [66]:

$$C_\varepsilon = \max\{R : P_{out}(R) \le \varepsilon\} \tag{76}$$

Similar to the derivation procedure of ergodic capacity, we take Rayleigh fading channel as an example to illustrate the details of outage capacity and outage probability. From the analysis above, it is not difficult to find that the randomness of outage capacity is caused by the randomness of the channel attenuation factor $|r|$, which is a Rayleigh distributed random variable. Hence, according to (75), we have:

$$
\begin{aligned}
P_{out}(R) &= \Pr\left[\log\left(1+\frac{|r|^2 P_{tr}}{N_0}\right) < R\right] \\
&= \Pr\left[|r|^2 < \left(1+\frac{(2^R-1)N_0}{P_r}\right)\right] \\
&= \Pr\left[-\sqrt{\frac{(2^R-1)N_0}{P_r}} < |r| < \sqrt{\frac{(2^R-1)N_0}{P_r}}\right] \\
&= \Pr\left[0 < |r| < \sqrt{\frac{(2^R-1)N_0}{P_r}}\right] \\
&= \int_0^{\sqrt{\frac{(2^R-1)N_0}{P_r}}} \frac{|r|}{\sigma^2} e^{-\frac{|r|^2}{2\sigma^2}} d|r| \\
&= 1-e^{\frac{(2^R-1)N_0}{2\sigma^2 P_{tr}}}
\end{aligned}
\tag{77}
$$

Because of the assumption $P_r = P_t = 2\sigma^2 P_t = P_{tr}$, we have $2\sigma^2 = 1$. Consequently, (77) can be further reduced to:

$$P_{out}(R) = 1-e^{\frac{(2^R-1)N_0}{2\sigma^2 P_{tr}}} \tag{78}$$

Moreover, solving (78) yields the maximum transmission rate $R_{\max}$, i.e. the outage capacity C_ε when the outage probability threshold ε is given:

$$C_\varepsilon = R_{\max} = \log\left[1-\frac{P_{tr}}{N_0}\ln(1-\varepsilon)\right] \tag{79}$$

In order to enlarge the outage capacity, we can employ diversity techniques. Assuming L diversity channels are involved and following (33), (40), and (78), we can determine the outage probability in this scenario by [8]:

$$P_{out-L}(R) = 1-e^{\frac{(2^R-1)N_0}{P_{tr}}} \sum_{k=0}^{L-1} \frac{1}{k!}\left[\frac{(2^R-1)N_0}{P_{tr}}\right]^k \tag{80}$$

If we let $P_{out-L}(R) = \varepsilon$, we can obtain the maximum transmission rate, i.e. the outage capacity for the diversity-based case as well. However, because (80) is a transcendental equation, there is no closed expression of C_ε [67]. By some approximation methods, a numerical solution could be provided [68]–[70].

D. Coding Techniques Associated with Fading Channels

As we can see from Section III, diversity techniques are very powerful to overcome the negative effects of fading. From the viewpoint of coding, diversity techniques can be regarded as coding techniques as well, because the original information is encoded into a number of replicas. To further improve the system performance, we might involve more sophisticated codewords to interleave the information bits in time-frequency space [8]. Such a digital communication system considering coding can be depicted in Fig. 20.

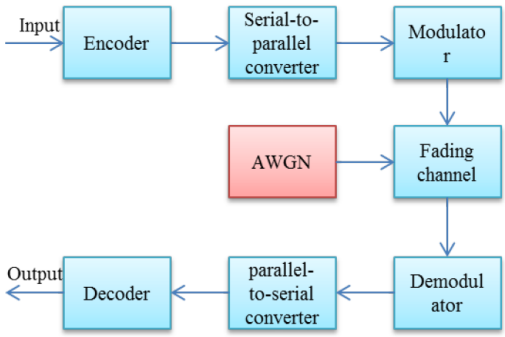

Fig. 20. Digital communication system considering coding [8].

VI. Conclusions

In conclusion, the relevant properties and techniques of fading and fading channels are reviewed in this paper. Specifically, we have analyzed the characterization and classification of fading channels. Then, four types of commonly used fading channels, their unique time/frequency domain properties and applicability are introduced. With simulations, we have also discussed the performance of signals propagating over flat and slow fading channels. By the simulation results, we are able to observe the effects of fading on signal propagation. Moreover, in order to overcome the negative impact of fading, diversity techniques have been expatiated and the communication system with and without diversity are simulated and compared. The feasibility and wide applicability of diversity can be validated by these simulation results.

In addition, several signaling techniques, including wideband signaling, RAKE demodulation and OFDM, are presented with a series of mathematical derivations and explanations. Finally, we have delved into the information-theoretical issues relevant to fading channels and addressed several important concepts to investigate into the essence of fading. Therefore, a number of potential research directions as stated above have been revealed. By reading this paper, the readers are expected to have a broad understanding of fading phenomenon, a variety of types of fading channels, effects of fading on wireless communication and the methodologies to overcome the disadvantageous effects.

Moreover, through the review over a large amount of contents, we would also like to point out a series of potential research directions which are worth further investigating in the future. They are summarized as follows:

- Channel modeling considering pass loss, shadowing and small-scale fading comprehensively.
- Fading channel modeling of multihop systems and multicarrier systems.
- Fading analysis and explanation from the perspective of electromagnetism.
- Design and test of receivers' prototypes which are able to handle deep fading scenario and recover the signals.

- Fading channel modeling considering location distribution of communication nodes over random networks.
- Fading channel modeling of self-organized networks and considering mutual interference.

REFERENCES

[1] D. Tse and P. Viswanath, *Fundamentals of Wireless Communication*, New York, NY, USA: Cambridge University Press, 2005.

[2] I. Rpke, T. H. Christensen, and J. O. Jensen, "Information and communication technologies: A new round of household electrification," *Energy Policy*, vol. 38, no. 4, pp. 1764–1773, 2010.

[3] P. Barsocchi, "Channel models for terrestrial wireless communications: A survey," CNR-ISTI Technical Report, 2006.

[4] H. Hashemi, "The indoor radio propagation channel," *Proceedings of the IEEE*, vol. 81, no. 7, pp. 943–968, Jul. 1993.

[5] M. Simon and M. Alouini, Digital Communication over Fading Channels, ser, Wiley Series in Telecommunications and Signal Processing, Wiley, 2005.

[6] G. Sheng, S. Dang, N. Hossain, and X. Zhang, "Modeling of mobile communication systems by electromagnetic theory in the direct and single reflected propagation scenario," in *Applications and Techniques in Information Security*, Springer Berlin Heidelberg, 2015, pp. 280–290.

[7] D. Cox and R. Leck, "Distributions of multipath delay spread and average excess delay for 910-MHz urban mobile radio paths," *IEEE Transactions on Antennas and Propagation*, vol. 23, no. 2, pp. 206–213, Mar. 1975.

[8] J. Proakis and M. Salehi, *Digital Communications*, McGraw-Hill Education, 2007.

[9] T. Rappaport, *Wireless Communications: Principles and Practice*, 2nd ed. Upper Saddle River, NJ, USA: Prentice Hall PTR, 2001.

[10] M. Li, J. Tan, and W. Zhang, "A channel estimation method based on frequency-domain pilots and time-domain processing for OFDM systems," *IEEE Transactions on Consumer Electronics*, vol. 50, no. 4, pp. 1049–1057, Nov. 2004.

[11] G. Eluma and K. Arshad, "Indoor statistical channel modelling using Agilent 8960," in *Proc. International Conference on Current Trends in Information Technology (CTIT)*, Dec. 2013, pp. 265–269.

[12] J. Jethva and M. Porwal, "MIMO detectors comparison for its BER performance in various channels," in *Proc. International Conference on Advances in Electrical Engineering*, Jan. 2014, pp. 1–6.

[13] S. P. Dang, M. Zhang, J. Ridge, J. Bristow, and A. Gholamzadeh, "Conceptual design of wireless anti-theft alarm system based on antenna array and wave transmission model," in *Applied Mechanics and Materials*, 2015, pp. 818–825.

[14] F. Mahmood, F. Abdullah, and H. Al-Tayyar, "Analysis, simulation and modeling of mobile Rayleigh fading channel using Labview," in *Proc. Loughborough Antennas and Propagation Conference*, Nov. 2011, pp. 1–6.

[15] C. C. Chong, Y. Kim, and S. S. Lee, "A modified S-V clustering channel model for the UWB indoor residential environment," in *Proc. IEEE 61st Vehicular Technology Conference*, vol. 1, May 2005, pp. 58–62.

[16] B. Hashem and E. Sousa, "Performance of cellular DS/CDMA systems employing power control under slow RICIAN/Rayleigh fading channels," in *Proc. IEEE 5th International Symposium on Spread Spectrum Techniques and Applications*, Sep. 1998, vol. 2, pp. 425–429.

[17] K. J. Yang, C. L. Wang, and Y. R. Tsai, "Joint channel and Doppler spread estimation over time-varying flat-fading channels," in *Proc. IEEE 75th Vehicular Technology Conference*, May 2012, pp. 1–5.

[18] P. Gaydecki, Foundations of Digital Signal Processing: Theory, Algorithms and Hardware Design, ser. IEE Circuits, Devices and Systems Series, 2004.

[19] D. So, *Lecture Notes of Digital Mobile Communications*, The University of Manchester, 2014.

[20] K. Witrisal, Y. H. Kim, and R. Prasad, "Frequency-domain simulation and analysis of the frequency-selective RICEAN fading radio channel," in *Proc. Ninth IEEE International Symposium on Personal, Indoor and Mobile Radio Communications*, 1998, vol. 3, pp. 1131–1135.

[21] L. Ros and E. P. Simon, "Second-order modeling for Rayleigh flat fading channel estimation with Kalman filter," in *Proc. 17th International Conference on Digital Signal Processing*, July 2011, pp. 1–6.

[22] F. L. Chiu, N. Y. Yu, and G. Gong, "Maximum correlation of binary signals over fading channels," in *Proc. International Symposium on Information Theory*, Sept. 2005, pp. 1913–1917.

[23] Y. Yan, C. Gan, C. Zuo, S. Wu, and S. Dang, "Analysis of uniform and optimal power allocation strategies for decode-and-forward relay considering direct transmit link," in *Proc. International Conference on Electrical and Information Technologies*, Mar. 2015, pp. 425–429.

[24] P. L. Yeoh, M. Elkashlan, and I. Collings, "Mimo relaying: Distributed TAS/MRC in Nakagami-m fading," *IEEE Transactions on Communications*, vol. 59, no. 10, pp. 2678–2682, Oct. 2011.

[25] G. Prabhu and P. Mohana Shankar, "Simulation of flat fading using MATLAB for classroom instruction," *IEEE Transactions on Education*, vol. 45, no. 1, pp. 19–25, Feb. 2002.

[26] F. Davarian, "Fade margin calculation for channels impaired by RICIAN fading," *IEEE Transactions on Vehicular Technology*, vol. 34, no. 1, pp. 41–44, Feb. 1985.

[27] W. Rummler, "A new selective fading model: Application to propagation data," *Bell System Technical Journal*, vol. 58, no. 5, pp. 1037–1071, May 1979.

[28] H. J. Park, K. W. Lee, and Y. H. Lee, "Channel estimation with dedicated pilot signal in MIMO-OFDM systems," in *Proc. IEEE 73rd Vehicular Technology Conference*, May 2011, pp. 1–5.

[29] N. Shariati, J. Wang, and M. Bengtsson, "Robust training sequence design for correlated MIMO channel estimation," *IEEE Transactions on Signal Processing*, vol. 62, no. 1, pp. 107–120, Jan 2014.

[30] A. Aghamohammadi and H. Meyr, "On the error probability of linearly modulated signals on Rayleigh frequency-flat fading channels," *IEEE Transactions on Communications*, vol. 38, no. 11, pp. 1966–1970, Nov. 1990.

[31] Z. Ma, A. Gholamzadeh, B. Tang, S. Dang, and S. Yang, "Matlab based simulation of the efficiency of the complex OFDM on power line communication technology," in *Proc. Fourth International Conference on Instrumentation and Measurement, Computer, Communication and Control*, Sept. 2014, pp. 374–378.

[32] K. Yan, Y. Yang, and S. Dang, "A SVD-based optimum algorithm research for macro-femtocell interference coordination," in *Proc. IEEE 81st Vehicular Technology Conference*, May 2015, pp. 1–6.

[33] Z. Sheng, *Probability and Statistics*. Beijing, China: Higher Education Press, 2008.
[34] M. Fozunbal, S. McLaughlin, and R. Schafer, "On space-time-frequency coding over MIMO-OFDM systems," *IEEE Transactions on Wireless Communications*, vol. 4, no. 1, pp. 320–331, Jan 2005.
[35] J. Lindner, "MIMO-OFDM: Basic relations between coding, spreading, multicarrier and singlecarrier transmission," in *Proc. 6th IEE International Conference on 3G and Beyond*, Nov. 2005, pp. 1–1.
[36] L. Silveira, F. Assis, and E. Pinto, "Performance of a psk system with wavelet time diversity over flat Rayleigh fading channels," in *Proc. SBMO/IEEE MTT-S International Microwave and Optoelectronics Conference*, 2003, vol. 1, pp. 187–191.
[37] A. Molisch and M. Win, "MIMO systems with antenna selection," *IEEE Microwave Magazine*, vol. 5, no. 1, pp. 46–56, Mar. 2004.
[38] R. Price and P. Green, "A communication technique for multipath channels," *Proceedings of the IRE*, vol. 46, no. 3, pp. 555–570, Mar. 1958.
[39] S. Dang, J. Coon, and D. Simmons, "Combined bulk and per-tone relay selection in super dense wireless networks," in *Proc. IEEE International Conference on Communication Workshop*, Jun. 2015, pp. 2200–2205.
[40] P. Guo, Y. Bai, Z. Ma, S. Wu, and S. Dang, "Relay technology for multicarrier systems: A research overview," in *Proc. Third International Conference on Computer, Communication, Control and Information Technology*, Feb. 2015, pp. 1–5.
[41] A. Annamalai and C. Tellambura, "Analysis of hybrid selection/maximal-ratio diversity combiners with gaussian errors," *IEEE Transactions on Wireless Communications*, vol. 1, no. 3, pp. 498–511, Jul. 2002.
[42] B. Ouarzazi, M. Berbineau, I. Dayoub, and A. Menhaj-Rivenq, "Channel estimation of OFDM system for high data rate communications on mobile environments," in *Proc. 9th International Conference on Intelligent Transport Systems Telecommunications*, (ITST), Oct. 2009, pp. 425–429.
[43] A. Nasri, R. Schober, and L. Lampe, "Performance of BICM-OFDM systems in UWB interference," *IEEE Transactions on Wireless Communications*, vol. 8, no. 9, pp. 4389–4392, Sept. 2009.
[44] S. Nawaz, S. Mohsin, and A. Ikaram, "Neural network based MIMO-OFDM channel equalizer using comb-type pilot arrangement," in *Proc. International Conference on Future Computer and Communication*. Apr. 2009, pp. 36–41.
[45] P. Bello and B. Nelin, "The effect of frequency selective fading on the binary error probabilities of incoherent and differentially coherent matched filter receivers," *IEEE Transactions on Communications Systems*, vol. 11, no. 2, pp. 170–186, June 1963.
[46] S. Mason, C. Berger, S. Zhou, and P. Willett, "Detection, synchronization, and Doppler scale estimation with multicarrier waveforms in underwater acoustic communication," *IEEE Journal on Selected Areas in Communications*, vol. 26, no. 9, pp. 1638–1649, Dec. 2008.
[47] C. Fan and L. Cao, *Principles of Communications*, Beijing, China: National Defence Industry Press, 2006.
[48] C. Xiao and Y. Zheng, "On the ergodic capacity of mimo triply selective rayleigh fading channels," *IEEE Transactions on Wireless Communications*, vol. 7, no. 6, pp. 2272–2279, June 2008.
[49] C. Xiao and Y. R. Zheng, "Ergodic capacity of mimo triply selective rayleigh fading channels," in *Proc. Global Telecommunications Conference*, Nov. 2004, vol. 5, pp. 3133–3137.
[50] L. Li and A. Goldsmith, "Capacity and optimal resource allocation for fading broadcast channels .ii. outage capacity," *IEEE Transactions on Information Theory*, vol. 47, no. 3, pp. 1103–1127, Mar 2001.
[51] L. Li and A. Goldsmith, "Outage capacities of broadcast fading channels with channel side information under different spectrum-sharing techniques," in *Proc. Communication Theory Mini-Conference*, Jun. 1999, pp. 27–31.
[52] C. Potter, K. Kosbar, and A. Panagos, "Multiple-input multiple-output Rayleigh flat fading outage capacity using channel estimation," in *Proc. IEEE Radio and Wireless Symposium*, Jan. 2008, pp. 575–578.
[53] Z. X. Ma, M. Zhang, S. Shaham, S. P. Dang, and J. Hart, "Literature review of the communication technology and signal processing methodology based on the smart grid," in *Applied Mechanics and Materials*, 2015, vol. 719, pp. 436–442.
[54] S. Shamai and T. Marzetta, "Multiuser capacity in block fading with no channel state information," in *Proc. IEEE International Symposium on Information Theory*, 2000.
[55] O. Al-Askary and S. Slimane, "Effect of error in channel state information on the channel capacity with QAM signalling and the design of robust signal constellations," *IET Communications*, vol. 1, no. 6, pp. 1118–1125, Dec. 2007.
[56] G. Caire and S. Shamai, "On the capacity of some channels with channel state information," *IEEE Transactions on Information Theory*, vol. 45, no. 6, pp. 2007–2019, Sep. 1999.
[57] T. Cover and M. Chiang, "Duality between channel capacity and rate distortion with two-sided state information," *IEEE Transactions on Information Theory*, vol. 48, no. 6, pp. 1629–1638, Jun. 2002.
[58] M. Souryal and R. Pickholtz, "Adaptive modulation with imperfect channel information in OFDM," in *Proc. IEEE International Conference on Communications*, 2001, vol. 6, pp. 1861–1865.
[59] B. Larrousse and S. Lasaulce, "Coded power control: Performance analysis," in *Proc. IEEE International Symposium on Information Theory*, July 2013, pp. 3040–3044.
[60] R. You, H. Li, and Y. Bar-Ness, "Diversity combining with imperfect channel estimation," *IEEE Transactions on Communications*, vol. 53, no. 10, pp. 1655–1662, Oct 2005.
[61] T. Cover and J. Thomas, *Elements of Information Theory, ser. A*, Wiley-Interscience Publication Wiley, 2006.
[62] D. Dalalah, L. Cheng, and G. Tonkay, "Modeling end-to-end wireless lossy channels: A finite-state markov approach," *IEEE Transactions on Wireless Communications*, vol. 7, no. 4, pp. 1236–1243, Apr. 2008.
[63] G. Caire and S. Shamai, "On the capacity of some channels with channel state information," in *Proc. IEEE International Symposium on Information Theory*, Aug. 1998.
[64] G. Taricco and M. Elia, "Capacity of fading channel with no side information," *Electronics Letters*, vol. 33, no. 16, pp. 1368–1370, Jul. 1997.
[65] S. Choudhury and J. Gibson, "Information transmission over fading channels," in *Proc. IEEE Global Telecommunications Conference*, Nov. 2007, pp. 3316–3321.
[66] L. Ozarow, S. Shamai, and A. Wyner, "Information theoretic considerations for cellular mobile radio," *IEEE Transactions on Vehicular Technology*, vol. 43, no. 2, pp.

359–378, May 1994.
[67] Y. Liu, *Calculus*, Science Press, 2010.
[68] R. Hasan and M. Hafez, "Outage capacity of best relay selection protocol for cooperative wireless networks over nonidentical Nakagamim channels with arbitrary *m*," in *Proc. 6th International Conference on Wireless and Mobile Communications*, Sept. 2010, pp. 404–409.
[69] C. H. Lee, C. J. Chang, and W. H. Sheen, "A capacity analysis method for uplinks in DS/CDMA cellular systems with imperfect sir-based power control and multipath fading," *IEEE Transactions on Wireless Communications*, vol. 7, no. 1, pp. 78–83, Jan. 2008.
[70] Z. Li, L. Jia, F. Li, and H. Hu, "Outage performance analysis in relay-assisted inter-vehicular communications over double-Rayleigh fading channels," in *Proc. International Conference on Communications and Mobile Computing*, April 2010, vol. 2, pp. 266–270.

Zhongli Wang graduated from Beihua University and University of Science and Technology Beijing for the majors of Communication Engineering and Control Theory & Control Engineering, respectively. He is currently an associate professor with College of Electrical and Information Engineering, Beihua University and dedicates to the investigations of pattern recognition and embedded systems. He has tens of papers published in international journals and proceedings and wrote three textbooks. He also participated in two research projects sponsored by National Natural Science Foundation of China, four research projects sponsored by the local municipal government, and three research projects sponsored by his university.

Guo Sheng graduated from Zhejiang University, is the associate professor with Zhejiang Post and Telecommunication College. He has published several papers related to the research into electronics and communication engineering. His current research interests include electronics, wireless communication and signal processing.

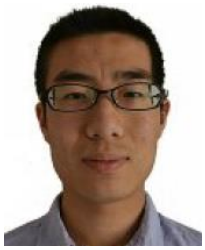

Xu Zhang received the BS degree from Department of Mechanical Engineering and Materials Science, University of Shanghai for Science and Technology, Shanghai, China. He is now a fourth year PhD candidate at Department of MEMS, Duke University. His research interests include artificial intelligence, neural networks, neurorobotics.